International Journal of Rock Mechanics & Mining Sciences 62 (2013) 42–50

Contents lists available at SciVerse ScienceDirect

International Journal of Rock Mechanics & Mining Sciences

journal homepage: www.elsevier.com/locate/ijrmms

Creep closure rate of a shallow salt cavern at Gellenoncourt, France

B. Brouard [a], P. Bérest [b,*], V. de Greef [b], J.F. Béraud [b], C. Lheur [c], E. Hertz [c]

[a] Brouard Consulting, 101 rue du Temple, 75003 Paris, France
[b] Laboratoire de Mécanique des Solides, Ecole Polytechnique Paris Tech, 91128 Palaiseau, France
[c] Compagnie des Salins du Midi et des Salines de l'Est, 137 rue Victor Hugo, Levallois Perret, France

ARTICLE INFO

Article history:
Received 26 July 2011
Received in revised form
10 October 2012
Accepted 25 December 2012
Available online 11 May 2013

Keywords:
Mechanical behavior of salt
Creep closure
Cavern abandonment

ABSTRACT

Cavern creep closure rate was recorded in the SG13–SG14 salt cavern of the Gellenoncourt brine field operated by CSME at Gellenoncourt in Lorraine, France. Cavern compressibility and the evolution of cavern brine temperature first were measured. In this shallow cavern (250-m, or 800-ft, deep), which had been kept idle for 30 years, cavern-brine thermal expansion can be disregarded. To assess cavern closure rate, a 10-month brine-outflow test was performed, followed by a 6-month shut-in test. During the tests, brine outflow or pressure evolution is influenced by atmospheric pressure changes, ground temperature changes and Earth tides. From the average pressure-evolution rate, it can be inferred that the steady-state cavern closure rate is slower than 10^{-5}/year or 3×10^{-13}/s.

1. Introduction

Thousands of caverns have been leached out worldwide from salt formations. Their volumes range from 10,000 to more than 1,000,000 m^3, and their depths from 100 to 3000 m. In the long term, salt behaves as a viscous fluid and caverns gradually shrink. Deep caverns have experienced closure rates by several percent per year, as proved by direct measurement of cavern shape evolution through sonar survey. However sonar survey accuracy typically is 1% (when distance from cavern axis to cavern wall is concerned). In shallow caverns, sonar surveys are performed to measure cavern shape changes during solution mining; however they are not accurate enough to detect small volume changes due to creep closure, which is much slower than in deeper caverns. In fact, creep-closure rate of shallow caverns can be assessed through shut-in pressure tests and outflow tests. *Shut-in pressure tests* consist of closing the cavern and measuring the pressure evolution at the wellhead as a function of time [1,2]. *Outflow tests* consist of opening the cavern and measuring the flow of fluid (brine or hydrocarbon) expelled from the wellhead [3–5].

Performing these tests—especially the shut-in pressure test is relatively easy. However interpreting such tests is not straightforward: in addition to cavern creep closure, many phenomena can contribute to pressure build-up or liquid outflow. Some of these phenomena (ground temperature variations, atmospheric pressure variations, earth tides) do not lead to a systematic error (when averaged on a long enough period, their effects are nil), but other phenomena have a much larger influence. They include cavern brine warming or cooling, and, especially during shut-in pressure tests, casing leaks or brine micro-permeation through the cavern wall. Furthermore, even when a cavern has been kept idle for some time (several months or years) before performing a mechanical test, steady-state creep still is far from being reached. For these reasons, only a small number of fully-documented tests have been described in the literature. For instance Bérest et al. [6] measured a $\dot{\varepsilon}_{cr} = \dot{V}/V = -3 \times 10^{-4}$/year cavern closure rate in a 950-m deep cavern at Etrez, France; Brouard et al. [5] observed a $\dot{\varepsilon}_{cr} = \dot{V}/V = -10^{-3}$/year convergence rate in a 700-m deep cavern at Carresse, France.

In this paper, we describe a brine outflow test and a shut-in pressure test performed in a 250-m deep cavern of the Gellenoncourt brine-field operated by Compagnie des Salins du Midi et Salines de l'Est (CSME) in Lorraine, France. The objective of these tests was to assess long term cavern closure rate and its consequences from the point of view of environmental protection (ground subsidence and possible brine leaks to shallow water-bearing strata). Cavern closure rate in such a shallow cavern is exceedingly slow, which raises specific measurement problems.

2. The Gellenoncourt caverns

CSME has operated a brine field in Eastern France since 1965. This field includes the Gellenoncourt brine field, described in [7]. It is located at the eastern (and shallowest) edge of the Keuper bedded-salt formation of Lorraine–Champagne, in which the salt thickness is 150 m. Five horizontal sets of salt layers ("*faisceaux*", or bundles) have been described by geologists. The salt content of this field is highest in the first (shallowest) and third faisceaux. The overburden layers include argillite, dolomite, sandstone and limestone.

* Corresponding author. Tel.: +33 169335744; fax: +33 169335706.
E-mail address: berest@lms.polytechnique.fr (P. Bérest).

1365-1609/$ - see front matter © 2013 Published by Elsevier Ltd.
http://dx.doi.org/10.1016/j.ijrmms.2012.12.030

During the first half of the 20th Century, single wells were brined out. After 1965, the hydro-fracturing technique was used. For this brine field, cased and cemented wells are drilled to a depth of 280–300 m i.e., at the base of the third faisceau. The horizontal distance between two neighboring wells typically is 120–150 m. Through hydro-fracturing, a link is created between two such caverns at the base of the third pencil. Water then is injected in one well and brine is withdrawn from the other well. After some time, the injection and withdrawal wells are switched. The caverns grow, and their roofs actually reach the first pencil. Brining stops when the cavern roof is 10 m below the salt roof. This 10-m-thick salt slab is left to protect the overlying strata, which are prone to weathering when in contact with brine [7].

In 2007, CSME decided to perform tests to gain a better knowledge of cavern long-term mechanical behavior ("ACSSL" Project). The SG13–SG14 cavern was selected for performing in-situ tests, as this cavern is representative of the field and had been kept idle for a long period of time.

The SG13 and SG14 7"-wells were drilled in May 1975, and operated as brine-production caverns from July 1976 to June 1977 (SG13), and from October 1978 to July 1980 (SG14). After some time, the two caverns coalesced, and SG13–SG14 now is composed of two parts connected by a large link; hydraulically, they can be considered as a single cavern. A 3D view is provided in Fig. 1. From latest sonar measurements (2000), it was inferred that the volumes of SG13 and SG14 are 107,000 m^3 and 34,000 m^3, respectively. However, sonar measurements are likely to underestimate the overall cavern volume, as they cannot "see" the insoluble-filled link between the two caverns. Cavern volume at the end of the mining operations also can be inferred from "mass balance"; i.e., from the cumulated amounts of injected water and withdrawn brine during mining operations. "Mass balance" suggests that the actual cavern volume might be as large as $V \approx 240,000\ m^3$.

3. Cavern compressibility and cavern temperature measurement

3.1. Cavern compressibility measurement

Cavern compressibility, or βV, in m^3/MPa, is the ratio between the injected (or withdrawn) volume and the cavern pressure change during a rapid injection (or withdrawl). It is proportional to cavern volume, or V, and it is related to the elastic (adiabatic) properties of the rock mass and of the fluids contained in the cavern [8]. Let $q<0$ be the brine withdrawal flow-rate; cavern brine pressure decreases by $\dot{P}_c<0$, generating a $\dot{V}_b=-\beta_c V_c \dot{P}_c$ brine expansion rate and a $\dot{V}_c=\beta_c V_c \dot{P}_c$ cavern contraction rate. V_b and V_c are brine and cavern volumes, respectively; they experience very small changes and one can set $V_b \approx V_c \approx V$, however, when pressure evolution is concerned, these changes cannot be neglected, $\dot{V}_b \approx \beta_b V \dot{P}_c \dot{V}_c \approx \beta_c V \dot{P}_c$. As $q+\dot{V}_b=\dot{V}_c$, $q=\beta V \dot{P}$ and $\beta=\beta_b+\beta_c$ cavern, overall compressibility is the sum of brine compressibility and "hole-in-the-salt" compressibility. Typical values are $\beta_b=2.6\times10^{-4}$/MPa and $\beta_c=1.3\text{–}2\times10^{-4}$/MPa (depending on cavern shape and salt elastic properties), and in most caverns $\beta \approx 4\text{–}5\times10^{-4}$/MPa.

On June 3, 2008, the compressibility of the SG13–SG14 cavern was measured by depressurizing SG13 by $\Delta P_c \approx -0.07$ MPa. Cavern compressibility proved to be $\beta V=129.5\ m^3$/MPa. When "mass balance" cavern volume, which is $V \approx 240,000\ m^3$ (see Section 2) is considered, the cavern compressibility coefficient can be inferred to be $\beta=5.5\times10^{-4}$/MPa; this figure is slightly higher than usual but still credible since cavern compressibility is known to be higher in a somewhat flat cavern [8].

3.2. Cavern temperature measurement

Brine thermal contraction (or expansion) results from the gap between the temperature of the cavern brine and the geothermal temperature of the rock. When cavern brine is warmer than the rock mass, heat is transferred from the cavern to the rock mass through conduction, resulting in brine cooling. Brine cooling generates brine cavern contraction, making brine outflow rate or wellhead pressure rate slower. Brine thermal contraction (or expansion, when brine is cooler than the rock mass) effects during a shut-in test or a brine outflow test often are larger than the effects of cavern creep closure: in the following, it will be proven that the steady-state closure rate of the SG13–14 cavern is slower than $\dot{\varepsilon}_{cr} \approx -10^{-5}$/year. Brine thermal-expansion coefficient is $\alpha_b=4.4\times10^{-4}/^{\circ}$C. Even a brine temperature decrease rate as slow as $\dot{T}_c=-0.02^{\circ}\,C$/year would generate a relative brine volume decrease rate of $\alpha_b \dot{T}_c \approx -10^{-5}$/year i.e., of the same order of magnitude as that of the cavern creep closure rate. In other words,

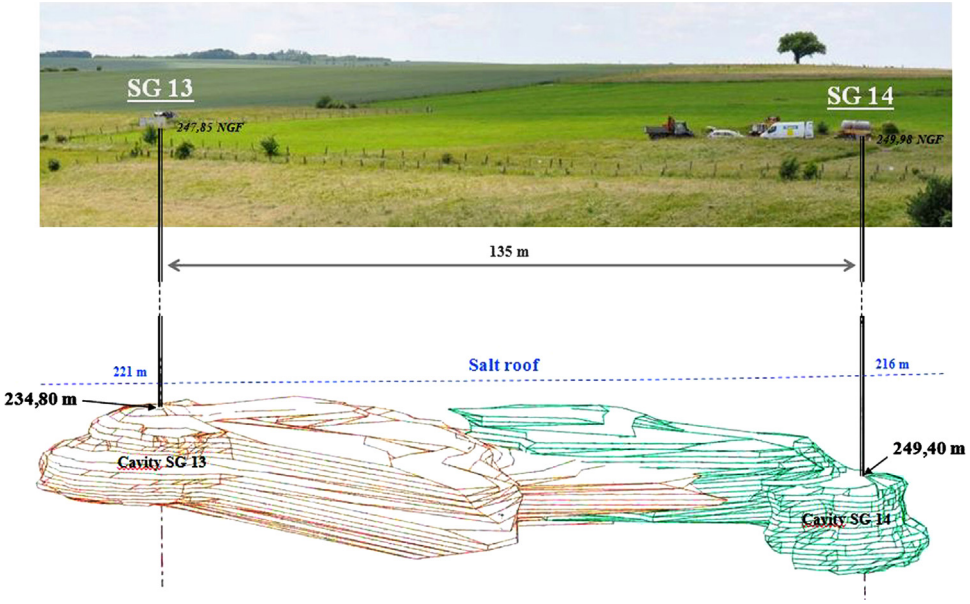

Fig. 1. 3D view of the SG13–SG14 cavern (From November 2000 sonar survey); the cavern is viewed from East to West with a 10° downward dip angle.

correct interpretation of a creep closure test requires that brine temperature changes are nil or that these changes can be assessed precisely.

The brine cooling process is slow—even slower in a larger cavern. In a cavern with volume $V=240{,}000\ m^3$, the temperature gap between rock mass temperature and brine cavern temperature which existed at the end of the leaching period is divided by a factor of 4 after 10 years [9]. For the SG13–SG14 cavern, soft water injected during the leaching process was slightly warmer (20 °C) than the geothermal temperature of the rock, which typically is $T_0(H)=17.5$ °C at cavern depth ($H=250$ m). The initial gap was small. Moreover, the cavern had been kept idle for nearly 30 years by the time the brine-outflow test began. It was believed that temperature decrease rate was exceedingly slow at that time.

By December 2008, a temperature gauge was lowered into the SG13 well to assess changes in brine cavern temperature. The cavern temperature was measured at a 247-m depth and remained perfectly constant during the period December 2008–November 2009. In June 2010, cavern temperature was measured again using the same gauge; gauge depth was 244 m (the small difference in gauge depth is not significant, as natural convection is active in the cavern and vertical temperature gradient in the cavern brine is small) and brine temperature was exactly the same as in December 2008. Gauge resolution was tested as follows: cavern pressure was increased by $\Delta P_c = 1$ MPa by injecting brine during one day. During such a short period of time, brine evolutions are almost perfectly adiabatic [9] and a $\Delta T_c = \alpha_b T_c \Delta P_c / \rho_b C_b$ temperature increase could be expected, where $T_c = 290$ K is the absolute brine temperature, $\rho_b C_b = 4.8 \times 10^6\ J/m^3/°C$ is the volumetric heat capacity of brine, or $\Delta T_c(°C) = 0.03 \Delta P_c$ (MPa). In fact, gauge temperature indication "jumped" by 0.02 °C when pressure increase had increased by $\Delta P_c \approx 0.6$ MPa proving that the gauge was sensitive and that its resolution was 0.02 °C. For the 18-month temperature measurement period, it can be inferred that temperature rate is slower than $|\dot{T}_c| = 0.013$ °C/year, possibly much slower, as the initial temperature gap was small in 1988, almost 30 years before the test.

4. The brine outflow test

4.1. Experimental set-up

A general view of the outflow measurement system is given in Fig. 2, left. A cabin was installed above the wellhead for security reasons, and a solar panel was set on the cabin roof to provide an energy supply, as the caverns are located far from the brine field station. Fig. 2 (left) shows the upper part of the 7" steel casing. A hole was drilled through the casing (Fig. 2, right) to allow evacuation of the out-flowing brine to a plastic container whose weight was measured every minute. When this container is filled with brine, an electric valve automatically triggers container venting. A plastic cylinder was set above the upper end of the 7" steel casing to prevent overflow. (After a rapid drop in atmospheric pressure, brine flow sometimes may be very fast, resulting in the rise of the air/brine interface above the hole for a couple of minutes, before overflowing brine is evacuated to the container through the hole, as explained below.)

4.2. Average brine flow-rate

In 2000 the cavern was shut-in after a sonar survey. Eight years later, before the test began, well head pressure had built up to approximately 0.08 MPa. On 3 July 2008, after the compressibility test (see Section 3.1) the cavern was opened and wellhead pressure dropped to zero. The outflow test began on 23 July 2008 and was completed by 25 May 2009; its duration was 306 days. In principle, the *average* brine outflow rate, or q, is governed by cavern-creep closure and cavern-brine thermal expansion:

$$q = -\dot{\varepsilon}_{cr} V + \alpha_b \dot{T}_c V \tag{1}$$

In the case of the SG13–SG14 cavern, it was proven (see Section 3.2) that brine thermal expansion rate is likely to be exceedingly slow ($\dot{T}_c \approx 0$). The same can be said of possible leaks, as wellhead pressure is zero during a liquid outflow test. Atmospheric pressure fluctuations, ground temperature fluctuations and Earth tides will be discussed in the next Section; they are more or less periodic phenomena and their *average* effect during a 10-month long test is negligible. Brine crystallization will be discussed in Section 6.4. In other words, the observed average flow-rate is representative of cavern creep closure during the test. The cumulated mass of expelled brine as a function of time, or $m(t) = \rho_b \nu(t)$, $\dot{\nu}(t) = q$ is shown in Fig. 3. The average brine-outflow rate (i.e., the overall amount of brine expelled during the testing period divided by the testing period duration) was 9.5 l/day. When this flow is compared to the cavern volume, or $V=240{,}000\ m^3$,the relative creep closure rate is $\dot{\varepsilon}_{cr} = -q/V = -4.6 \times 10^{-13}\ s^{-1} = -1.45 \times 10^{-5} year^{-1}$. However brine outflow clearly decreases during the test period; a part

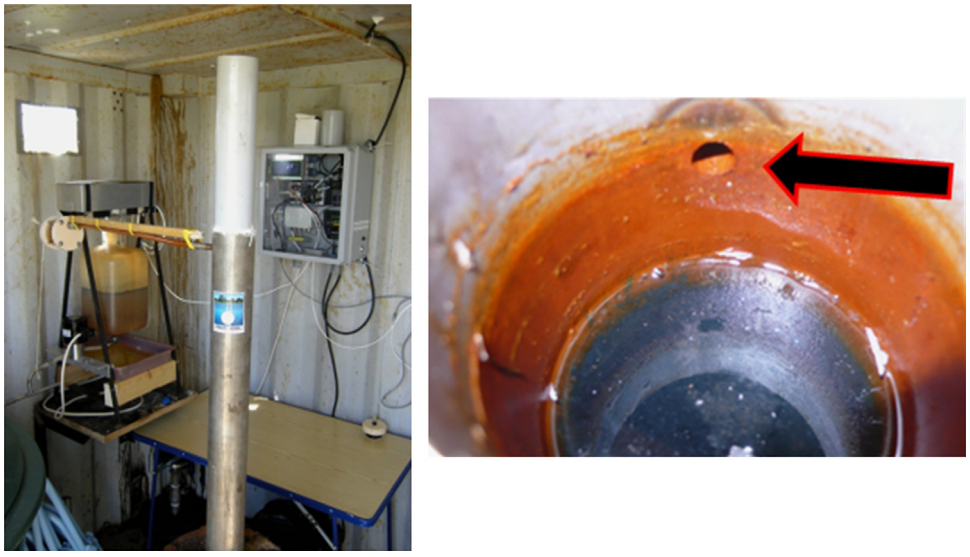

Fig. 2. Brine outflow measurement system (left) and venting hole in the 7" steel casing.

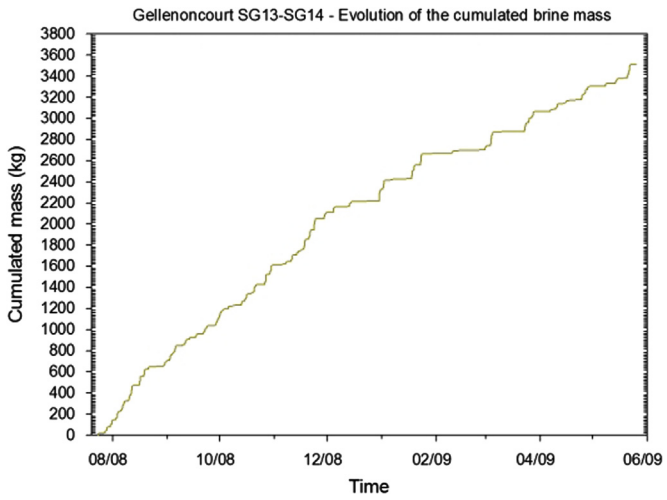

Fig. 3. Cumulated expelled mass as a function of time from 23 July 2008 to 25 May 2009.

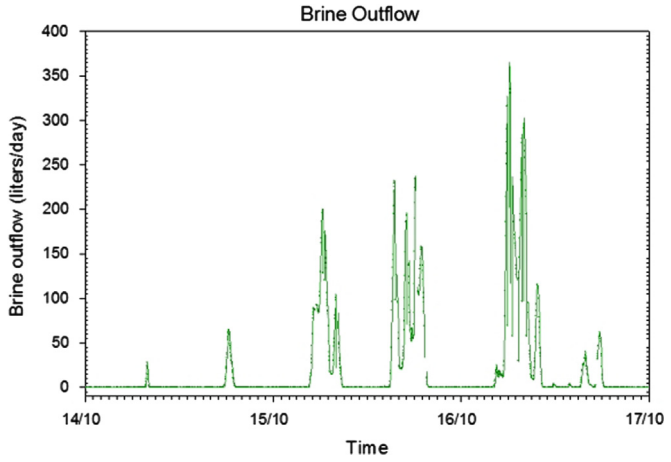

Fig. 4. Brine flow-rate as a function of time from 14 October to 17 October 2008. The average brine flow rate is computed every 10 min.

of the initial flow was triggered by the July-3 cavern pressure drop and is transient in nature. Steady-state creep closure rate is slower, see Section 6.

4.3. Brine flow-rate fluctuations

The *average* brine flow-rate was computed in Section 4.2. However, Fig. 3 shows that, in fact, the flow rate vanishes to zero during several-day-long periods. Fig. 4 displays flow-rate evolution during a three-day long period (from 14 October 2008 to 17 October 2008). Large fluctuations can be observed: periodically, the brine flow rate is several hundreds of liters per day i.e., larger than the average flow rate by one or two orders of magnitude. Conversely, for most of the time, the flow rate is nil: no flow is expelled from the cavern, and the air/brine interface drops down into the well. Several phenomena contribute to this apparently erratic behavior, among which the most significant is atmospheric pressure variations; they are discussed below.

4.3.1. Atmospheric pressure fluctuations

Let h be the height of the brine column (Fig. 5); cavern pressure, or P_c, and atmospheric pressure, or P_{atm}, are related by (2), where $\rho_b g$ is brine volumetric weight:

$$P_c = \int_0^h \rho_b g dz + P_{atm} \quad \text{or} \quad \dot{P}_c = \rho_b g \dot{h} + \dot{P}_{atm} \tag{2}$$

(Dynamic and thermal effects are neglected at this step). Two cases must be considered:

Brine is expelled from the cavern. When brine is expelled from the cavern, $h = H$, $\dot{h} = 0$ (Fig. 5, right) and the flow of brine, or $\boldsymbol{q}$ can be written as

$$q = -\dot{\varepsilon}_{cr} V + \beta_\infty V \dot{P}_{atm} - \beta V \dot{P}_c \tag{3}$$

where $-\beta_\infty V \dot{P}_{atm}$ is the cavern contraction rate generated by stress changes in the rock mass due to atmospheric pressure fluctuations and $-\beta_\infty V \dot{P}_c$is the brine expelled flow rate resulting from cavern pressure changes (which exactly equal atmospheric pressure changes, $\dot{P}_c = \dot{P}_{atm}$, when $h = H$). Atmospheric pressure experiences somewhat erratic fluctuations whose amplitude is several hPa. They are transmitted to the rock mass through the ground (and also through the brine column in the well). Except during a severe storm, pressure changes are almost uniform in a large horizontal domain whose dimensions are much larger than cavern depth (H=250 m). Hence, at such a depth, it can be assumed that the horizontal displacements generated by atmospheric pressure

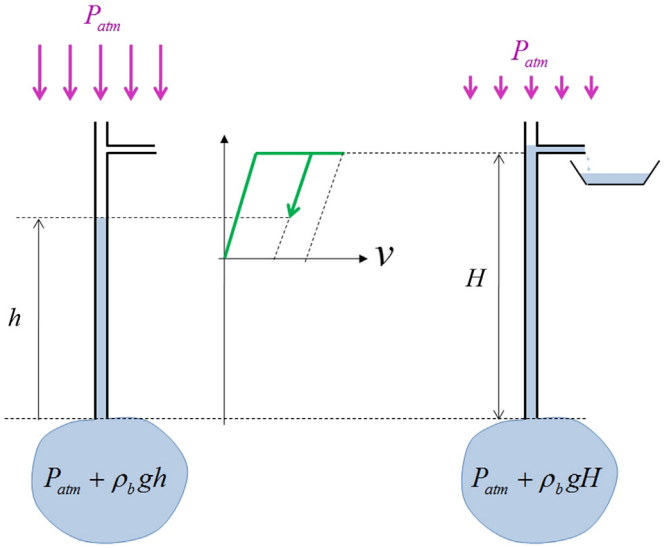

Fig. 5. Brine outflow from a shallow cavern: low atmospheric pressure and brine flow from the cavern (right); rapidly increasing atmospheric pressure with no observed brine flow (left). Note the analogy with an elasto-plastic system; ν is the cumulated volume of expelled brine, $\dot{\nu} = q$.

fluctuations are negligible and the additional stresses generated by these fluctuations are $\dot{\sigma}_{zz} = -\dot{P}_{at}$ and $\dot{\sigma}_{xx} = \dot{\sigma}_{yy} = -\bar{\nu}\dot{P}_{atm}/(1-\bar{\nu})$, where $\bar{\nu}$ is an equivalent Poisson's ratio for the rock mass between ground surface and cavern depth. These stresses generate a cavern-volume variation of $-\beta_\infty V \dot{P}_{atm}$ where β_∞ is a function of the elastic properties of the rock mass and of the shape of the cavern. In the case of an ideally spherical cavern, $\beta_\infty = 3(1+\bar{\nu})/2\bar{E}$. Combining (2) and (3) leads to:

$$q = -\dot{\varepsilon}_{cr} V - (\beta - \beta_\infty) V \dot{P}_{atm} \quad ; \quad h = H \tag{4}$$

The brine/air interface is below the venting hole. Conversely, when the brine/air interface is below the venting hole, $h < H$, (Fig. 5, left) and:

$$S\dot{h} = -\dot{\varepsilon}_{cr} V + \beta_\infty V \dot{P}_{atm} - \beta V \dot{P}_c \; ; \quad h < H \tag{5}$$

(The same equation holds when $h = H$ and $\dot{h} < 0$.) Combining Eqs. (2) and (5) leads to

$$(S + \beta V \rho_b g)\dot{h} = -\dot{\varepsilon}_{cr} V - (\beta - \beta_\infty) V \dot{P}_{atm} \; ; \quad h < H \tag{6}$$

where the cross-sectional area of the well, or $S=2.1\times10^{-2}$ m^2 is much smaller than $\beta V\rho_b g\approx1.56$ m^2. To a certain extent, $\chi=(\beta-\beta_\infty)/(\beta+S/\rho_b gV)<1$, or the ratio between the change in well brine level ($\dot{h}$) and the change in atmospheric pressure expressed in terms of equivalent brine height ($\dot{P}_{atm}/\rho_b g$), can be compared to the "barometric efficiency", a notion defined in wells tapped in aquifer layers [10]. It is interesting to notice that, from a mathematical point of view, Eqs. (4) and (5) are similar to the equations that describe an elasto-plastic system when $\dot{\nu}=q$ (the rate of brine expelled from the cavern to the container) is the "plastic strain rate",$h<H$ is the "plastic" criterion and $G=1/(S+\beta V\rho_b g)$ is the "elastic modulus" (Fig. 5).

These equations prove that the cavern should behave as an extremely sensitive barometer, as will be shown by the shut-in pressure test described in Section 5. Consider for instance the case when brine is expelled from the well to the container, or $h=H$. Eq. (4) predicts that a change in atmospheric pressure by $\dot{P}_{atm}$ generates a change in brine flow rate by $q=-(\beta-\beta_\infty)V\dot{P}_{atm}$. It will be proved in Section 5 that $\beta_\infty/\beta\approx0.542$, or q(liters/day)$\approx-6\,\dot{P}_{atm}$(hpa/day).On a short time-scale, erratic fluctuations of atmospheric pressure can be observed, typically a 30 Pa drop in a 30 s period due for instance to a sudden gust of wind. Such a drop generates an additional 1.8 l brine flow in a short period of time i.e., a dramatic increase in brine flow rate.

Atmospheric pressure fluctuations can be accurately measured and it was expected, before the test, that the brine outflow rate could easily be corrected from their effects. However data processing led to relatively poor results [11]. Several factors explain this disappointing result. They include oscillations of the brine column, brine cooling in the well, ground temperature fluctuations and earth tides. They are investigated in the next sections.

4.3.2. Dynamic oscillations of the brine column in the well

Rapid changes in pressure trigger oscillations of the brine column in the well. A simple model captures the main features of this dynamic phenomenon. Consider the case when $h=H$ (brine is expelled from the well). Eqs. (2) and (4) must be rewritten as follows. The mass of brine contained in the well is $\rho_b SH$. When this mass moves up and down in the well, its acceleration is $\gamma=\dot{q}/S$. When derivated with respect to time, Newton's law of motion can be written as

$$\dot{P}_c=\left[\rho_b g\dot{h}+\dot{P}_{atm}\right]+\rho_b H\ddot{q}/S \tag{7}$$

and the brine outflow from the cavern is

$$q=[-\dot{\varepsilon}_{cr}V+\beta_\infty V\dot{P}_{atm}]-\beta V\dot{P}_c \tag{8}$$

In the context of rapid oscillations, the terms between brackets can be disregarded. Eliminating cavern pressure between Eqs. (7) and (8) leads to a second order differential equation, $(S/\beta V)q+\rho_b H\ddot{q}=0$. This equation describes harmonic oscillations. As $\beta V\rho_b g\approx1.56$ m^2 and $S=2.1\times10^2$ m^2, the period of small oscillations is $\tau=2\pi\sqrt{H\beta V\rho_b/S}$, or 4 min. These oscillations are slowly dampened, [8], and they blur the relation between atmospheric pressure variations and brine outflow to the container.

4.3.3. Cooling of the brine column rising inside the well

When the well is at rest, cavern brine temperature, or T_c is warmer than brine temperature in the well, which is $T_0(z)=T_c-\Gamma z$; Γ is the geothermal gradient. When brine moves upward, cool brine expelled at ground level is substituted by warm brine flowing from the cavern and the brine column in the well is made lighter, cavern pressure decreases, and brine flow is made faster. However heat exchange in the well between the rock formation and the warm brine in the well must also be taken into account. It is assumed that outflow takes place, $h=H$; Eq. (2) must be re-written in the more precise form:

$$P_c=\int_0^H\rho_b g dz+P_{atm}\quad\text{and}$$

$$\dot{P}_c=\int_0^H\frac{\partial\rho_b}{\partial t}g dz+\dot{P}_{atm}=\rho_b g\alpha_b\int_0^H\frac{\partial T}{\partial t}dz+\dot{P}_{atm} \tag{9}$$

where $T(z,t)$ is brine temperature in the well. It is assumed that well brine was at rest when $t<0$;i.e, $q(t<0)=0$, and that its temperature equaled rock geothermal temperature, or $T(z,t<0)=T_0(z)$. When brine rises in the well, its temperature $T=T(z,t)$ is slightly warmer than rock temperature $T_R(r,z,t)$ at the same depth and heat exchange takes place. Heat flux from the rock mass should be described by Fourier's equation for heat conduction. As we are mainly interested in orders of magnitude, the following simplistic model is accepted: the heat flux is assumed to be proportional to the difference between rock virgin temperature and brine temperature:

$$\frac{dT(z,t)}{dt}\equiv\frac{\partial T}{\partial t}(z,t)+\frac{q}{S}\frac{\partial T}{\partial z}(z,t)=-\frac{1}{t_c}[T(z,t)-T_0(z,t)]$$

$$T(z,0)=T_0(z)=T_c-\Gamma z\quad;\quad T(0,t)=T_c \tag{10}$$

where a is the well radius, $t_c\approx a^2/k_{salt}$, $k_{salt}\approx100$ m^2/year is the thermal diffusivity of salt and $t_c=1$–2 h This partial differential equation must be solved according to the characteristic lines method. When brine flow rate or q is assumed to be approximately constant for any $t>0$, the solution of Eq. (10) is:

$$\begin{cases}T(z,t)=T_c-\Gamma z+\Gamma qt_c[1-\exp(-t/t_c)]/S & \text{when}\quad z-qt/S>0\\ T(z,t)=T_c-\Gamma z+\Gamma qt_c[1-\exp(-Sz/qt_c)]/S & \text{when}\quad z-qt/S<0\end{cases} \tag{11}$$

from which it can be inferred that

$$\int_0^H\frac{\partial T(z,t)}{\partial t}dz=\Gamma q\int_{qt/S}^H\exp(-t/t_c)dz/S=(H-qt/S)\Gamma q\exp(-t/t_c)/S$$

$$\text{when}\quad qt/S<H \tag{12}$$

This quantity is largest at $t=0$; at this instant, combining Eqs. (3), (9) and (12) leads to:

$$q(1-\beta V\rho_b g\alpha_b\Gamma H/S)=-\dot{\varepsilon}_{cr}V-(\beta-\beta_\infty)V\dot{P}_{atm} \tag{13}$$

where $\beta V=130$ m^3/MPa, $\Gamma=3\times10^{-2}$ °C/m, $S=2.1\times10^{-2}$ m^2, $H=250$ m, Eq. (13) proves that brine rate is significantly accelerated when warm cavern brine enters the well (note that this model predicts that, when a bigger and deeper cavern is considered—say $H=1000$ m and $\beta V=500$ m^3/MPa then $\beta V\rho_b g\alpha_b\Gamma H/S>1$ and the cavern+well system behaves as a geyser: from time to time, triggered by atmospheric pressure variations, puffs of brine are spewed from the cavern.)

4.3.4. Ground temperature fluctuations and Earth tides

They are not specific to the brine outflow test; their effects are relatively small in the context of a brine outflow test and they will be discussed in Section 5.

4.3.5. Conclusion

This analysis proves that, even if the average brine flowrate clearly is representative of cavern behavior, flowrate daily behavior is blurred by large fluctuations from external origin. Interpretation of the shut-in pressure test will prove to be simpler.

5. The shut-in pressure test

5.1. Average pressure build-up rate

The cavern was shut-in from 25 May 2009 to 19 November 2009 (178 days). During a shut-in test, Eqs. (1) and (2) which describe averaged evolutions must be re-written as

$$q = 0 = -\dot{\varepsilon}_{cr}V - \beta V\dot{P}_c, \quad \dot{P}_c = \dot{P}_{wh} \tag{14}$$

where P_{wh} is the wellhead pressure. Wellhead pressure evolution is shown on Fig. 6. Wellhead pressure increase during this 10-month period is 80 kPa, making the average pressure build-up rate due to cavern creep closure $\dot{P}_{wh} = \dot{\varepsilon}_{cr}/\beta \approx 47.1$ Pa/day. The cavern compressibility coefficient is $\beta \approx 5.4 \times 10^{-4}$/MPa (see Section 3.1), from which it can be inferred that cavern closure rate is $\dot{\varepsilon}_{cr} = \dot{V}/V \approx -0.93 \times 10^{-5}$/year and $\dot{\varepsilon}_{cr}V = -\beta V\dot{P} \approx -6.1$ l/day $= -2.2$ m^3/year

5.2. Wellhead pressure fluctuations

Even if a general trend can be observed clearly, wellhead pressure experiences significant fluctuations. For example, Fig. 7 displays wellhead pressure and atmospheric pressure as measured from 1 September 2009 to 3 November 2009. A striking correlation can be observed. The wellhead is closed; however atmospheric pressure fluctuations are transmitted to the cavern through the rock mass. Daily fluctuations in wellhead pressure are generated by daily changes in ground level temperature, which are transmitted through heat conduction/convection to a few meters below ground. The same can be said from seasonal fluctuations, which are transmitted deeper below ground. A wellhead temperature increase generates brine warming in the upper part of the well, brine expands, the brine column in the well becomes slightly lighter, and the *wellhead* pressure, or P^{wh}, increases. To take into account these phenomena, Eq. (14) must be re-written in the more precise form:

$$q = 0 = -\dot{\varepsilon}_{cr}V - \beta V\dot{P}_c + \beta_\infty V\dot{P}_{atm} + \alpha_b S\int_0^H \frac{\partial T}{\partial t}dz \tag{15}$$

$$\dot{P}_c = \dot{P}_{wh} - \alpha_b\rho_b g\int_0^H \frac{\partial T}{\partial t}dz \tag{16}$$

The value of the integral $\dot{I} = \int_0^H (\partial T/\partial t)dz$ is a couple of dozens of °C × m/day (it is larger when the well is filled with a liquid hydrocarbon rather than brine). Combining Eqs. (15) and (16)

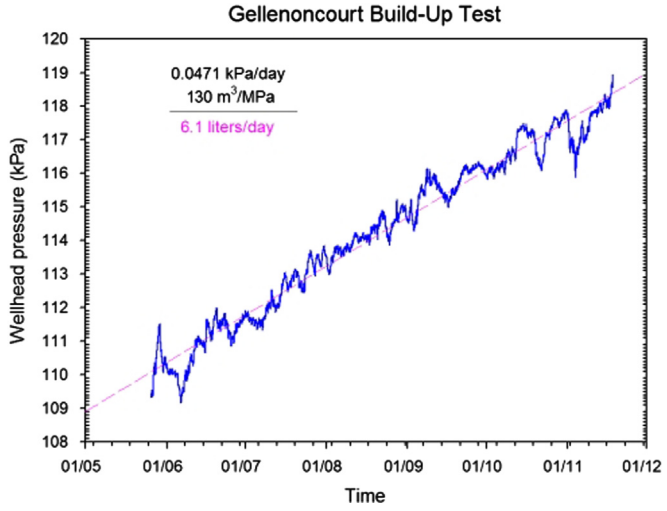

Fig. 6. Wellhead pressure evolution from 26 May 2009 to 18 November 2009 during the shut-in test.

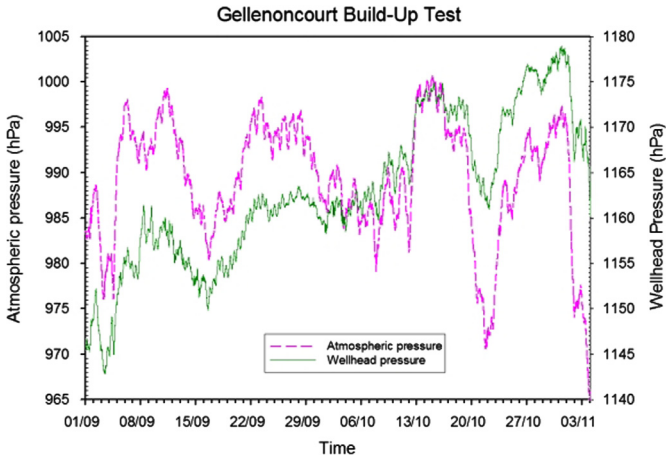

Fig. 7. Wellhead pressure and atmospheric pressure as measured during the September–November period.

leads to:

$$\dot{P}_{wh} = -\frac{\dot{\varepsilon}_{cr}}{\beta} + \frac{\beta_\infty}{\beta}\dot{P}_{atm} + \alpha_b\left(\rho_b g + \frac{S}{\beta V}\right)\dot{I} \tag{17}$$

Fig. 8 displays the wellhead pressure changes (upper-left picture) and atmospheric pressure changes (lower-left picture) as a function of time from 25 May 2009 to 19 November 2009. Ground-level temperatures also are shown in Fig. 8 (upper-right picture). We searched for an empirical correlation between wellhead pressure, atmospheric pressure evolutions and ground-level temperature changes of the following form:

$$P^{wh}(t) = P^{wh}(0) - \frac{\dot{\varepsilon}_{cr}t}{\beta} + \frac{\beta_\infty}{\beta}\left[P_{atm}(t) - \overline{P}_{atm}\right] + \alpha_b(\rho_b g + \frac{S}{\beta V})L\left[T^{wh}(t-\varphi) - \overline{T}_{atm}\right] \tag{18}$$

where $\dot{\varepsilon}_{cr}/\beta \approx -47.1$ Pa/day is the average wellhead-pressure increase rate; $I \approx [T_{atm}(t-\varphi) - \overline{T}_{atm}]$, where $\overline{T}_{atm}$ and $\overline{P}_{atm}$ are the average ground temperature and atmospheric pressure, respectively, φ is the time lag associated with heat transfer through the wellhead; L is a characteristic length, or the average depth of penetration of atmospheric temperature changes (a few meters) $L, \beta_\infty/\beta$ and φ are three constants to be determined empirically. When corrected from atmospheric pressure and temperature variations, wellhead pressure evolution as a function of time is much smoother (Fig. 8, lower-right picture). The effects of ground temperature variations are small. The coefficient of correlation between cavern pressure variations and atmospheric pressure variations is $\beta_\infty/\beta \approx 0.542$, which means that approximately 54% of atmospheric pressure variations are transmitted to cavern brine through the rock mass. A Fourier analysis also was performed (Fig. 9) and two peaks clearly can be observed. Corresponding periods are 12 h 25 min and 24 h, strongly suggesting that these peaks are associated with the effects of Earth tides. In fact, fluctuations generated by Earth tides are visible clearly on Fig. 7, for instance between September 15 and September 25, a period during which their amplitude is $\Delta P^{wh} \approx 1$ hPa from which it can be inferred that cavern deformation is $\beta\Delta P^{wh} \approx 5 \times 10^{-8}$, a figure that is typical of the strains induced by Earth tides [12,13].

6. Steady-state cavern creep vs. transient cavern creep

6.1. Closure rate decrease during the outflow test

It was observed during the brine outflow test that the *average* brine flow rate, computed from July 23, 2008 to May 25, 2009, was: $q/V = 4.6 \times 10^{-13}$ s^{-1} $= 1.45 \times 10^{-5}$ year^{-1} During the shut-in test, from 25 May 2009 to 19 November 2009 the cavern creep

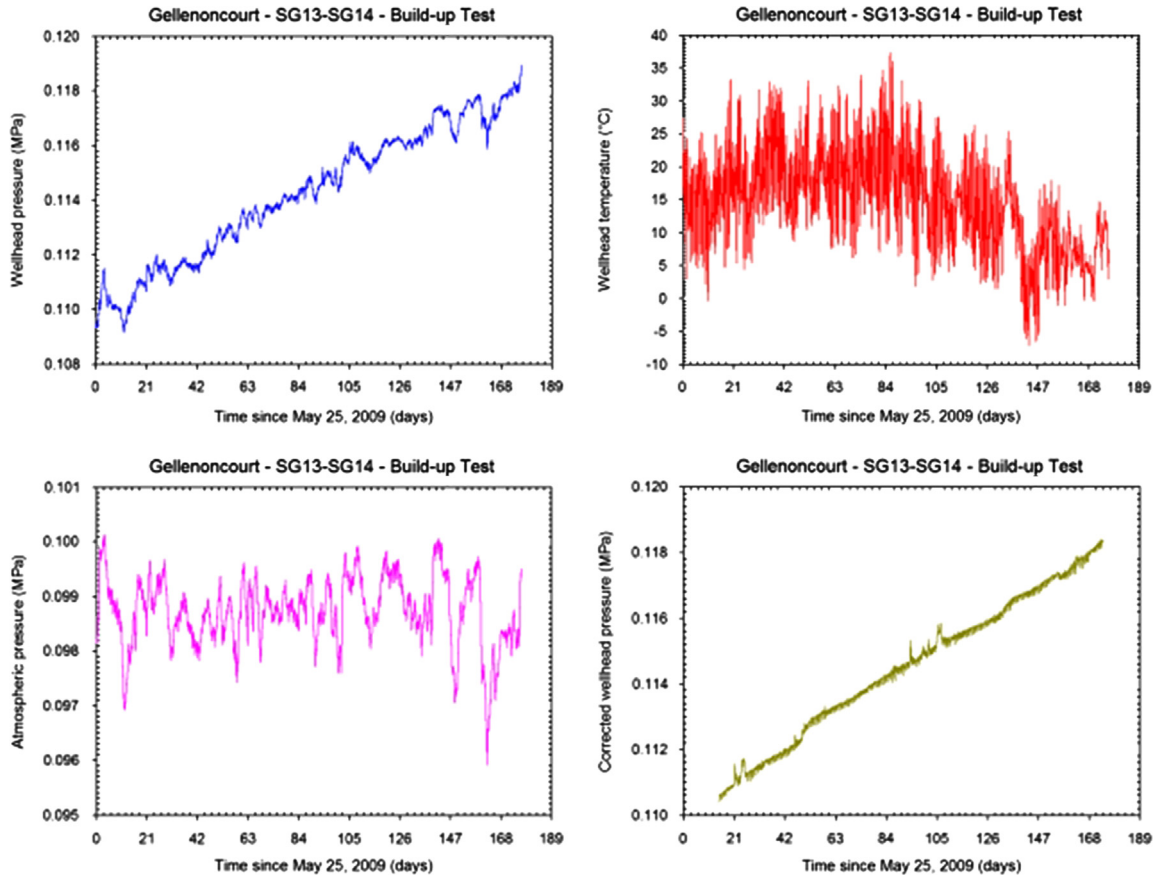

Fig. 8. Measured pressure (top left), atmospheric pressure (bottom left), atmospheric temperature (top right) and corrected pressure (bottom right).

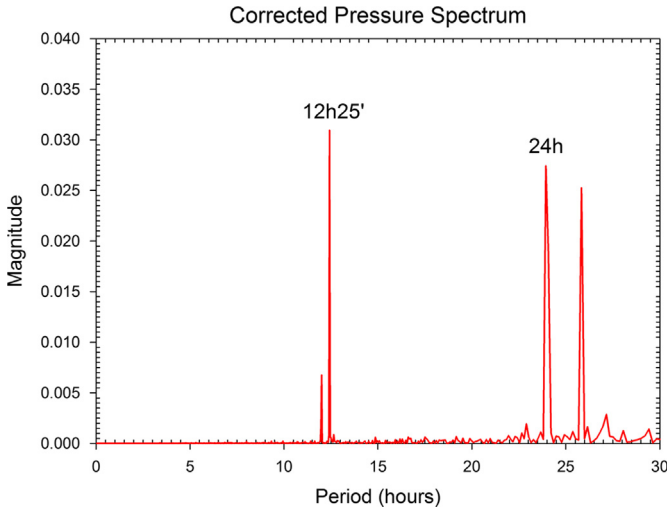

Fig. 9. Spectrum of corrected pressure minus trend.

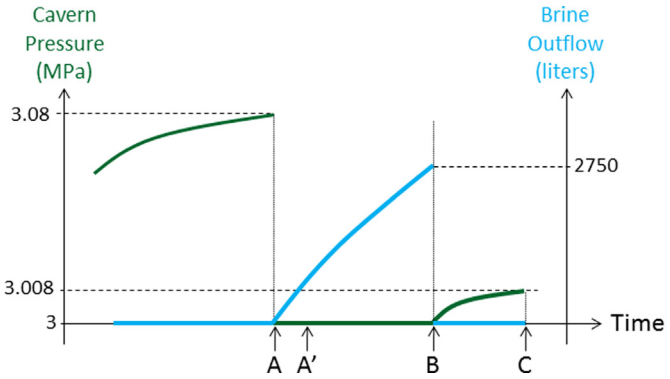

Fig. 10. The cavern was shut-in in 2000 and opened from 3 June 2008 (A) to 25 May 2009 (B) when it was shut-in again to 19 November 2009 (C). The brine outflow test begins on 23 July 2008 (A'). Transient phenomena triggered by rapid pressure drop are expected to play a role during the brine outflow test (A' B).

closure rate, inferred from pressure increase rate, was slower, $-\dot{\varepsilon}_{cr} = -\dot{V}/V = \dot{P}/\beta \approx 2.9 \times 10^{-13}\,s^{-1} = 0.93 \times 10^{-5}$ year^{-1}

Fig. 11 displays both the average rate $\overline{q}(t)$ computed on a 1-month period ("running" average) as a function of time during the outflow test and the average rate $\overline{\overline{q}}(t)$ computed since the beginning of the outflow test:

$$\overline{q}(t) = \frac{1}{30}\int_{t-15}^{t+15} q(\tau)d\tau \ (t \text{ in days}) \quad \overline{\overline{q}}(t) = \frac{1}{t}\int_{0}^{t} q(\tau)d\tau \tag{19}$$

This first average rate, or $\overline{q}(t)$, is somewhat erratic, as expected, as the flow-rate experiences large fluctuations originating in atmospheric pressure changes; however a gradual decrease can be observed. This is clearly confirmed by the evolution of the second average flowrate, or $\overline{\overline{q}}(t)$, which slowly decreases to reach its final value or 9.5 l/day at the end of the test.

It was seen on Fig. 3 that the cumulated expelled volume during the 306-day long outflow test was $v = 2750$ l (brine density is 1200 kg/m^3). During the shut-in test, the average cavern volume loss rate is 6.1 l/day, equivalent to 1865 l during a 306 day-long period. The difference, or 2750

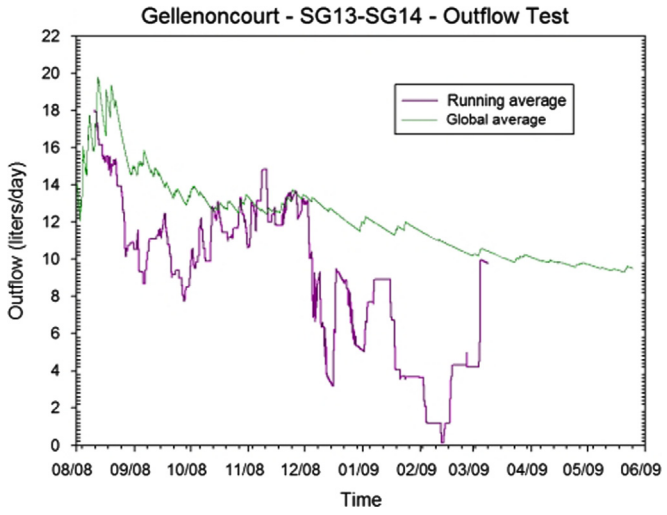

Fig. 11. Evolution of brine outflow—running average computed on a 1-month long period and average outflow since the beginning of the test.

−1865 = 885 l, can be explained by the effects of several transient phenomena [14].

It was mentioned that the cavern had been shut-in from 2000 to 2008; on 3 June 2008, when the compressibility test started, the wellhead (relative) pressure dropped by slightly more than $\Delta P_c = -0.08$ MPa (Fig. 10). In the SG13–SG14 cavern, the brine pressure at cavern depth is $P_c \approx 3$ MPa,and the gap between geostatic pressure and cavern pressure is $P_\infty - P_c \approx 2.5$ MPa. A wellhead pressure drop of $\Delta P_c = -0.08$ Mpa generates an increase of this gap by $\Delta P_c/(P_\infty - P_c) = 3.2\,\%$ a small figure, but large enough to trigger various transient phenomena, including: brine warming, transient brine permeation, salt crystallization and transient creep. They are discussed in the following.

It must be noticed that these transient phenomena were active immediately after the June 3 pressure drop (Fig. 10A) and their effects were especially significant during the 50-day long period before the brine flow test began on July 23 (Fig. 10A'). These effects are not included in the overall 855-l transient brine outflow observed during the outflow test.

6.2. Brine warming

The pressure drop by $\Delta P_c = -0.08$ MPa generates an adiabatic temperature decrease by $\Delta T_c = \alpha_b T_c \Delta P_c/\rho_b C_b \approx -0.002\ ^\circ C$,too small a drop to be detected by the temperature gauge (see Section 3.2). This drop is followed by an exceedingly slow brine warming which, after several years, generates an overall $\alpha_b V \Delta T_c = T_c \Delta P_c/\rho_b C_b \approx 210$ l brine volume increase. Even if brine warming is relatively fast during the first weeks following the pressure drop, the brine volume increase rate is too slow to play a significant role.

6.3. Brine permeation and leaks

During the 6-month long shut-in test, pressure increased by 0.008 MPa. If such a rate was sustained during an eight-year long period, pressure build-up should be 0.128 MPa, i.e. larger than the pressure increase observed during the 2000–2008 period, which was 0.08 MPa. This discrepancy can reasonably be attributed to the effects of creep closure deceleration and to the effects of micro-leaks and brine permeation, which are larger when cavern pressure is higher. Note that such leaks exist only when natural pore pressure in the rock mass—a quantity which is poorly known is smaller than brine pressure in the cavern and well. Brine permeation to the rock mass is a reversible process and it can be expected that after cavern pressure suddenly dropped down, some of this seeped brine flowed back to the cavern.

6.4. Crystallization

Immediately after the pressure drop by $\Delta P_c = -0.08$ MPa, cavern brine is over-saturated in the new pressure conditions and crystallization takes place. After some time, saturation is reached again and brine density and brine concentration have decreased by $\Delta\rho_b = \rho_b a_s \Delta P_c$ and $\Delta c = c\psi \Delta P_c$, respectively (Brine concentration is the ratio between the salt mass and the salt +water mass in a given volume of brine). Let $\Delta V_c < 0$ the volume of crystallized salt (in this context cavern creep closure is disregarded) and $\Delta V^{\exp} > 0$ the volume of brine expelled from the cavern because of brine crystallization; V_b is the volume of brine in the cavern+the volume of expelled brine and $\Delta V_b = \Delta V_c + \Delta V^{\exp}$. The salt-mass and brine-mass conservation equations can write:

$$\rho_{salt}\Delta V_c = \frac{d}{dt}(\rho_b V_b) = \rho_b V_b a_s \Delta P_c + \rho_b \Delta V_b \tag{20}$$

$$\rho_{salt}\Delta V_c = \frac{d}{dt}(\rho_b c V_b) = \rho_b V_b c(a_s + \psi)\Delta P_c + \rho_b c \Delta V_b \tag{21}$$

From this system it can be inferred that:

$$\Delta V^{\exp} = \frac{c}{(1-c)} V_b \left[-\psi + \rho_b(a_s + \psi - c a_s)/\rho_{salt}\right] \tag{22}$$

Typical values of the parameters are [14] $c = 0.26$, $\rho_b = 1200$ kg/m^3, $\rho_{salt} = 2160$ kg/m^3, $\psi = 2.6 \times 10^{-4}$/MPa, $a_s = 3.16 \times 10^{-4}$/ MPa, and the volume of brine expelled as a consequence of crystallization is $\Delta V^{\exp} \approx 1200$ l. The kinetics of salt crystallization is difficult to compute; however a significant part of it certainly took place during the June 3 to July 23 period, i.e., before the brine flow test began.

6.5. Transient creep

During a uni-axial compressive creep test performed in the laboratory, any rapid change in the applied load triggers transient creep. In fact most authors consider that the observed strain rate is the sum of an (instantaneous) thermo-elastic strain, a transient strain and a steady-state strain:

$$\dot{\varepsilon} = \frac{\dot{\sigma}}{E_{salt}} + \alpha_{salt}\dot{T} + \dot{\varepsilon}^{tr} + \dot{\varepsilon}^{ss} \tag{23}$$

where E_{salt} is the salt Young's modulus; α_{salt} is the thermal expansion coefficient of salt; $\dot{\varepsilon}^{ss}$is the steady-state strain rate, observed when temperature and load are kept constant for a long period of time; $\dot{\varepsilon}^{tr}$ is the ("rheological") transient strain rate, which is triggered by any change in the applied load and vanishes after a couple of weeks or months when the load is kept constant. A simple formulation for steady-state strain rate is the power law, or Norton–Hoff law: $\dot{\varepsilon}^{ss} = A\exp(-Q/RT)\sigma^n$,where A, $Q/R$and n are three empirical constants (more advanced formulations can be found in the literature). Various transient creep laws were proposed in the literature; see for instance [15].

Cavern creep closure can be described by a similar expression:

$$\dot{V}_c/V| = \beta_c \dot{P}_c + \dot{V}_c/V|^{tr} + \dot{V}_c/V|^{ss} \tag{24}$$

Remarkably, rock thermal expansion only plays a minute role in this context [9]. When Norton–Hoff law is accepted, in the case of an idealized spherical cavern, steady-state cavern closure rate can

be written as

$$\dot{V}/V|^{ss} \approx -\frac{3}{2} A \exp\left(-\frac{Q}{RT}\right) \left[\frac{3(P_\infty - P_c)}{2n}\right]^n \quad (25)$$

The driving force for cavern creep-closure is the gap between the geostatic pressure (P_∞)and the cavern fluid pressure (P_c)at cavern depth. The main difference between a uniaxial formulation and a formulation relevant to the case of a cavern lays in the transient behavior of the cavern. Any change in cavern pressure triggers transient cavern closure or expansion creep. However, even if a part of this transient behavior is due, as expected, to the "rheological" transient behavior of the rock mass, a large part of it is due to the slow redistribution of stresses in the rock mass following any pressure change ("geometrical" transient behavior), an effect which is not present in the case of a uniformly loaded sample, as proved in [14]. "Geometrical" transient behavior can have a significant effect during a long period of time, several decades when the pressure change which triggered transient creep was large.

Consider again the case of an idealized spherical cavern. Computations are easier when $\nu_{salt} = 0.5$ is assumed. It is assumed that steady-state has been reached. Cavern pressure is decreased abruptly by a small amount ΔP_c. It can be proved that immediately after this pressure change cavern volume loss rate increases by:

$$\Delta(\dot{V}/V) = \left(\frac{n^3}{2n-1}\right)\left(\frac{\Delta P_c}{P_\infty - P_c}\right) \times \dot{V}/V|^{ss} \quad (26)$$

A small decrease in cavern pressure by, say, $\Delta P_c/(P_\infty - P_c) \approx -4\%$ generates a transient increase in cavern creep closure rate by $\Delta\dot{V}/\dot{V} \approx 56\%$ when $n=3$. For instance if the steady-state cavern closure rate is 6 l/day, the transient closure rate can be expected to be 9 l/day immediately after the pressure drop. It must be noticed that this simple assessment does not take into account the *rheological* transient behavior of salt; in other words, in an actual cavern, the increase in cavern closure rate may be significantly larger.

It was said in Section 6.1 that transient phenomena were responsible for a 885-l expulsion of brine during the brine outflow test. It was estimated that crystallization alone is responsible for a 1200-l expulsion; however a large part of the crystallization process took place before the brine flow test began. Transient creep closure and a possible brine back-flow from the rock mass to the cavern also may play a role. It is difficult to achieve a more precise assessment; qualitatively, transient phenomena can explain the discrepancy between the results of the brine flow test and the results of the shut-in test.

7. Consequences for long-term behavior of the cavern

It can be assumed that, before abandonment, cavern wells will be effectively plugged [16]. If this plug remains effective, even in the very long term, no brine leak will take place and a tiny amount of brine will seep to the salt formation. Cavern brine pressure will reach an equilibrium value, intermediate between geostatic pressure and halmostatic pressure (which is the cavern pressure when the well is filled with saturated brine and opened at ground level), such that cavern convergence rate is balanced exactly by the small brine flow permeating to the rock mass [6]. At this stage of the study, salt permeability has not been assessed, and equilibrium pressure cannot be computed. However, it is clear that the cavern closure rate at equilibrium pressure will be exceedingly slow and that this equilibrium pressure will be reached after a very long period of time (several dozens of centuries). If the plug becomes ineffective (a kind of a worst-case scenario), brine will flow from the cavern to the overlying strata. An upper bound of the leak flow rate is $\beta V \dot{P}_c = 130\ \mathrm{m^3/MPa} \times 47\ \mathrm{Pa/day} \times 365\ \mathrm{days} \approx 2.2\ \mathrm{m^3/year}$,a small value. In both cases, ground subsidence will be exceedingly slow.

8. Conclusions

A 10-month long brine outflow test and a 6-month long shut-in test were performed in a 250-m deep salt cavern at Gellenoncourt in Lorraine, France. Cavern volume approximately was 240,000 m^3. This cavern had been kept idle for 30 years before the tests and brine temperature changes were exceedingly small during the tests.

During the brine outflow test, atmospheric pressure fluctuations generate large erratic changes in the expelled brine flow rate, as the cavern behaves as an extremely sensitive barometer. These perturbations are much smaller during the shut-in test and small effects such that fluctuations in wellhead pressure generated by Earth tides can clearly be observed. From hindsight, it is clear that several phenomena associated with fluid flow in the well make detailed interpretation of a brine outflow test more difficult than the interpretation of a shut-in test, during which no movement of the liquids contained in the well takes place.

A few days before the test began, the cavern was decompressed by 0.08 MPa. Even if small, this pressure drop triggered a transient creep closure whose effects were clearly observed during the outflow test.

The steady-state creep closure rate, as observed during the shut-in test, is slightly slower than 10^{-5}/year or 2 m^3/year. This value proves that even in the long term (several centuries) subsidence and possible brine leaks from the cavern should have negligible impact from the point of view of environmental protection.

References

[1] Bérest P, Brouard B, Durup G. Shut-in pressure tests—case studies. In: Proceedings of SMRI fall meeting, San Antonio, Texas; 2000: p. 105–26.

[2] Van Sambeek L, Fossum A, Callahan G, Ratigan J. Salt mechanics: empirical and theoretical developments. In: Proceedings of 7th symposium on salt. Amsterdam, Elsevier; 1993: p. 127–34.

[3] Clerc-Renaud A, Dubois D. Long-term Operation of underground storage in salt. In: Proceedings of the 5th symposium on salt, Coogan AH, Hauber L, editors, the Salt Institute, vol. II; 1980: p. 3–10.

[4] Hugout B. Mechanical behavior of salt cavities—in situ tests—model for calculating the cavity volume evolution. In: Proceedings of 2nd conference on the mechanical behavior of salt, Hannover. Clausthal–Zellerfeld, Trans Tech Pub; 1988: p. 291–310.

[5] Brouard B, Bérest P, Héas JY, Fourmaintraux D, de Laguérie P, You T. An in situ test in advance of abandoning of a salt cavern. In: Proceedings of SMRI fall meeting, Berlin; 2004: p. 45–64.

[6] Bérest P, Bergues J, Brouard B, Durup JG, Guerber B. A salt-cavern abandonment test. Int J Rock Mech Min Sci 2001;38:343–55.

[7] Buffet A. The collapse of Compagnie des Salins SG4 and SG5 drillings. In: Proceedings of SMRI fall meeting, Rome; 1998: p. 79–105.

[8] Bérest P, Bergues J, Brouard B. Review of static and dynamic compressibility issues relating to deep underground salt caverns. Int J Rock Mech Min Sci 1999;36:1031–49.

[9] Karimi-Jafari M, Bérest P, Brouard B. Thermal effects in salt caverns. In: Proceedings of SMRI Spring Meeting, Basel; 2007: p. 166–77.

[10] Jacob CE. On the flow of water in an elastic artesian aquifer. Eos, Trans Am Geophys Union 1940;21:574–86.

[11] Brouard B, Hertz E, Lheur C, Bérest P, de Greef V, Béraud JF. A brine outflow test in Gellenoncourt caverns. In: Proceedings of SMRI spring meeting, Krakow; 2009: p. 105–20.

[12] Bérest P, Blum PA, Durup G. Effect of the moon on underground caverns. In: Proceedings of 33rd US symposium on rock mechanics, Santa Fe; 1992: p. 421–8.

[13] Brouard B. On the behavior of solution-mined caverns (in French). PhD Thesis, Ecole Polytechnique, France: 1998.

[14] Bérest P, Brouard B, Karimi-Jafari M, Van Sambeek L. Transient behavior of salt caverns—interpretation of mechanical integrity tests. Int J Rock Mech Min Sci 2007;44:767–86.

[15] Munson D, De Vries KL, Fossum AF, Callahan GD. Extension of the *M–D* model for treating stress drop in salt. In: Proceedings of 3rd conference on the mechanical behavior of salt, Palaiseau, France. Clausthal–Zellerfeld, Trans Tech Pub; 1993: p. 31–44.

[16] Crotogino F, Kepplinger J. Cavern well abandonment techniques guidelines manual. Report 2006-3 for the SMRI: 2006.